

Final Report for the
DESIGN OF A SOLAR SAIL MISSION TO MARS

A design project by students in the Department of Aerospace Engineering at Auburn University under the sponsorship of the NASA/USRA University Advanced Design Program.

Auburn University
Auburn University, Alabama
June 1989

N2SW-4435

(NASA-CR-186045) DESIGN OF A SOLAR SAIL
MISSION TO MARS Final Report (Auburn Univ.)
61 p CSCL 22A

N90-11771

Unclass
63/12 0241476

*... Continuing Education
is Essential ...*



Aerospace Engineering AE 449

Auburn University

Auburn, Alabama

Design of a Solar Sail Mission to Mars

Submitted to: Dr. J.O. Nichols

Submitted by: Richard Eastridge
Kerry Funston
Aminat Okia
Joan Waldrop
Christopher Zimmerman

Date Submitted: May 5, 1989

ABSTRACT

An evaluation of the design of the solar sail includes key areas such as structures, sail deployment, space environmental effects, materials, power systems, telemetry, communications, attitude control, thermal control, and trajectory analysis. Deployment and material constraints determine the basic structure of the sail, while the trajectory of the sail influences the choice of telemetry, communications, and attitude control systems. The thermal control system of the sail for the structures and electronics takes into account the effects of the space environment. Included also are a cost, and weight estimate for the sail.

TABLE OF CONTENTS

<u>Section</u>	<u>Page</u>
ABSTRACT	ii
LIST OF FIGURES	iv
LIST OF TABLES	v
INTRODUCTION	1
STRUCTURES	2
SAIL DEPLOYMENT	4
SPACE ENVIRONMENTAL EFFECTS	5
MATERIALS	7
POWER SYSTEMS	11
ATTITUDE CONTROL	13
COMMUNICATION	15
THERMAL CONTROL	15
TRAJECTORY	16
AUXILIARY PROPULSION	18
COST ESTIMATE	20
WEIGHT ESTIMATES	21
DESIGN SUMMARY	22
LIST OF REFERENCES	23

LIST OF FIGURES

<u>Figure</u>	<u>Title</u>	<u>Page</u>
1	Two-View Drawing of the Solar Sail	26
2	Cross-Sectional View of the Sail Bus	27
3	Solar Forces on a Reflective Surface	28
4	Solar Constant vs. Radius	29
5	Solar Force vs. Radius	30
6	Acceleration of the Sail vs. Radius	31
7	Velocity of the Sail vs. Radius	32
8	A Comparison of Metallized Kapton with and without a Chromium Coating	33
9	A Basic Spacecraft Power System	34
10	GaAs and Silicon Solar Cell Efficiency vs. Operating Temperatures	35
11	Titan IV Characteristics	36
12	Departure Phase Angle for Mars Intercept	37
13	Interplanetary Trajectory for Constant Sail Angle Showing Interception of Martian Orbit.	38
14	Schematic of Ball-Lock-Bolt Separation Mechanism	39
15	Kinematics of Ball-Lock-Bolt Separation System	40
16	Arrangement of Gas-Generator and Ball-Lock- Bolt Separation System for the Sail Bus	41

LIST OF TABLES

<u>Table</u>	<u>Title</u>	<u>Page</u>
1a	Thermal Properties of Various Spacecraft Materials	43
1b	Mechanical Properties of Various Spacecraft Materials	44
2	Properties of Unidirectional Advanced Composites	47
3	Comparison of Vehicle Separation Mechanisms	45
4	Characteristics of Some Solid Propellants	46
5a	Properties of Kapton	48
5b	Strength of Kapton	48
6a	Epoxy Resin F263 Properties	49
6b	Epoxy Resin F263 Availability	50
6c	Carbon Fabric Physical Properties	51
6d	Carbon Fabric Laminate Mechanical Properties	52
7	Characteristics of Different Storage Cells	53
8	General Electric Nickel-Cadmium Satellite Cells	54

DESIGN OF A SOLAR SAIL MISSION TO MARS

Introduction

A new area of interest in space vehicles is the solar sail. Various applications for which the solar sail has been considered since the 1950's are: attitude control of satellites, focusing light on the jungles of Vietnam, and a Halley's comet rendezvous. Although, for various reasons none of these projects were completed, new interest in solar sails has recently arisen. The solar sail is an alternative to the traditional rocket propelled space vehicle as an interplanetary cargo vehicle, and manufacture of solar sails on the space station is under consideration. Solar sails have several advantages over the traditional rocket, including an unlimited power supply, thus eliminating the need for refueling. Another advantage is the low maintenance needed.

The purpose of this project will be to design a solar sail mission to Mars. The vehicle will efficiently journey to Mars from a geosynchronous transfer orbit powered only by a solar sail. The vehicle will weigh 487.16 kg and will be launchable as a secondary payload on an expendable launch vehicle.

The project includes an investigation of various options to minimize cost, weight, and time of flight in order to determine the feasibility of the solar sail. The design of the sail and its deployment system are a major part of the project, as is the actual mission planning for the flight of the vehicle. Various

topics researched include solar power, material characteristics, space environments, thermal control, trajectories, and orbital maneuvers. Various configurations and stability characteristics are considered in order to determine the optimal structure of the vehicle. Another design consideration is the control system of the vehicle. This system includes the control of the attitude of the sail and communication between the satellite and the Deep Space Network. Various options for these systems are considered.

This project will aid in determining the feasibility of a solar sail vehicle and will also raise public interest in space research.

Structures

There are many aspects of the solar sail vehicle to consider in the design of the actual structure of the vehicle including the sail configuration, stability, the method of stiffening, and the housing for the various systems.

Designing the actual sail of the solar sail vehicle included consideration of several configurations. These involved various separated panels such as the helio-gyro vehicle considered for a Halley's Comet rendezvous and uniform panels such as the square sail chosen for this project. The square sail, as seen in figure 1, was chosen for several reasons. The simplicity of deployment of the square configuration is a major advantage as is its high area to mass ratio which is desirable to maximize power and speed. (1:7-9) This design consists of four graphite epoxy

booms, 114 m in length, connected tangentially to a cylindrical bus measuring 1.4 m in diameter and 1 m in length (see figure 2). The sail has four triangular sections contained between the booms and has a total area of 25,992 m². (2:16) The weight limitation determined the final measurements of the sail, and the total force (210,040.00 N/m²), on the bus determined the thickness of the bus at 1 cm. This thickness includes a large increase from the necessary thickness calculated to insure reliability. The total force calculated uses the material values in tables 1a and 2.

The method of stiffening the structure is also an important design consideration. Spinning the sail after deployment was not feasible because of complications in attitude control. Extendable booms were also considered but required mechanisms for extension which were undesirable because of the weight limitation. A free sail without booms was considered but lacked sturdiness for such a long trip with such varied conditions. Uncured booms were chosen for their flexibility and compactness in the uncured state with curing taking place after deployment. (1:4, 5)

Deployment

One of the major design considerations for the solar sail vehicle is the method of deploying the sail. Minimizing weight and complexity of the deployment system are primary concerns in designing the method of deployment.

The sail folds accordion style into a wedge shape between the booms. Both the sail and the booms will coil 26 times around the bus before deployment, and remain encased in a 1 mm thick open-ended aluminum alloy cylinder until deployed. The enclosed solar sail vehicle will be set into orbit spinning with an initial angular velocity of 100 rpm by an expendable launch vehicle. The casing will slide off with the small rocket used to initially escape earth orbit. The sail will then deploy due to the force of the spinning motion and the strain energy in the sail and boom material. (2:16) A damping system is necessary in order to stop the sail from spinning once it is fully deployed. This is necessary in order to simplify the attitude control of the sail and also to insure that the booms do not experience undue stress and strain at the attachment points to the bus. The sail will experience an angular velocity of .782 rpm when fully deployed and the attitude control system will stop the final spin.

Space Environmental Effects

There are several aspects of the space environment that influence the solar sail. The space environment is composed of electrically neutral ionized plasma. Although the gas is ionized, it remains neutral because it contains approximately the same number of free electrons and positive ions. Therefore, the very nature of this plasma makes it difficult to operate the solar sail. Some environmental phenomenon affecting operations are electromagnetic radiation, solar particle radiation, electrostatic charging, and micro-meteors.

The most significant characteristic of the space environment that will affect the solar sail is electromagnetic radiation. Although this type of radiation consists of a wide range of energy levels, the two of most importance are optical and ultraviolet radiation. Optical radiation is the sail's primary means of propulsion. As photons of light impact and reflect from the sail, they impart a certain momentum as illustrated in Figure 3. The momentum results in a normal force which is composed of an incidence force F_i and a reflective force F_r . The momentum causes an increase in pressure or force on one side of the sail resulting in acceleration. Optical radiation will affect the sail's acceleration, velocity, time in flight and rate of temperature increase. Ultraviolet radiation, on the other hand, will affect the materials of the solar sail.

A means of measuring solar radiation is the solar constant. The predominant energy level in solar radiation is optical

radiation because, although each proton carries a low amount of energy, there are a large amount of photons per area. The solar constant is the amount of energy, from all wave lengths, produced by the sun per second per square meter. (3:13) This constant changes inversely with the radius squared as seen in Figure 4. At Earth the constant is 1370.0 W/m² and reduces to 590.0 W/m² at Mars. (4:704-705)

The force on the sail is obtained from the solar constant. As photons of light impact the sail they cause a pressure increase. This pressure increase caused by the photons of light multiplied by the area determines the force. Figure 5 illustrates how the force decreases with increasing radius, and ranges from .23575 N at Earth to .10232 N at Mars. The force is derived under the assumption that the sail area equals the effective area. However, when the sail angles away from the sun and the effective area is different from the area, the force is then the pressure multiplied by the area and the cosine of the incidence angle.

Acceleration and velocity are the result of the force applied to the sail. The acceleration is simply the force divided by the mass and it ranges from .0005659 m/sec² at Earth to .0002437 m/sec² at Mars. Figure 6 illustrates how the acceleration decreases with increasing radius. The velocity, however, is the integral of the acceleration minus the effects of gravity, and ranges from 32.73 m/sec at Earth to 238.14 m/sec between Earth and Mars, as illustrated in Figure 7. (5:19-20)

The time of flight is dependent on the arc length and the velocity. Assuming an effective area equal to the sail area, the time of flight is 5.2 years. However, the sail will have to change its orientation to maintain its trajectory and thus the time of flight will be slightly increased.

The rate of temperature increase is dependent on the solar constant and the radius from the sun. The maximum temperature increase is .4466C/sec-m². The rate of temperature increase is used to determine which materials are used to radiate heat and maintain the temperature required for the electronics.

While ultraviolet radiation adds a small percentage to the acceleration, its main effect on the sail is to cure the booms after deployment. Of the radiation from the sun, 7% is ultraviolet radiation which is important to determine the time needed to cure the booms.

Solar particle radiation originates from the solar winds and consists of high energy free electrons, positive ions, and neutral particles. Its density is dependent on the sun's eleven year emission cycle. At the peak of its cycle, known as the solar maximum, the sun is emitting several tons of particles per second. The next solar maximum will occur in 1992 which coincides with the start of the mission and makes particle radiation a potential hazard. There are not many materials that are effective against particle radiation, therefore the sail will use redundant electrical systems.

Electrostatic charging is the buildup of a potential difference between the sail and the plasma in which it is immersed in the space environment. The photoelectric effect and plasma bombardment are two of the most common causes of electrostatic charging. Charging due to the photoelectric effect is produced by impact of photons on the outer surface of the sail. A method of prevention would be to rotate the sail, however, this will interfere with the sail's propulsion. The most feasible solution is to use as many conductive surfaces as possible and cover non-conducting surfaces with a conductor. The large surface area of the sail and its thin material make the problem of micro-meteor collisions a potential hazard. Paint chips, micro-meteors, and other particles ranging from micrometer to millimeter proportions present problems in the space environment due to the extremely high velocities of particles in space. The solution to the problem lies in the proper choice of materials. This topic will be discussed in greater detail in the materials section.

Materials

The consideration of solar sail materials is of primary importance because of the sail's extreme environment on the mission and also because the materials used will directly affect the sail performance. Specific environmental considerations include the effects of micrometeoroids on the material, the material's susceptibility to sustained radiation, and the

pliability of the material necessary for packing. Mass also is a large consideration because the lower the mass/area ratio of the sail, the faster the sail's acceleration. The optical properties of the sail affect acceleration; a high reflectivity and emissivity of the sail is essential for the effective transfer of momentum from the photons, as well as for thermal control of the sail film. Furthermore, the cost and availability of the sail materials must be taken into account.

The solar sail materials are classified into two parts: the actual sail materials and all structures reinforcing the sail and bus. The sail itself consists of several thin layers: a film base with a sun side coating to increase both reflectance and emittance and a back side coating to increase emittance.

The film chosen for the solar sail is a 2.0 μ m thickness of Kapton, a gold colored polyamide film made by Dupont which exhibits excellent qualities for this mission (see Tables 5a and 5b). It can withstand temperatures up to 350 degrees Celsius, has a thermal expansion of only 11.1×10^{-6} in/in/F, and has high resistance to tearing from micrometeoroids. Kapton is easy to metallize and when it is, it resists radiation. Furthermore, Kapton will fold and crease well, making it easy to pack in its pre-deployed state. (6:465)

The metallic coating of the sun side must exhibit several qualities. It must be electrically conductive, low in weight, able to give protection to the sail film from charged particles and from UV radiation. It also must be chemically and

mechanically stable to resist corrosion and withstand wide temperature ranges. The sail's film coating will be aluminum in a thickness of 1000 \AA , because it has these qualities. Aluminum will provide a high reflectance (.88) to reduce thermal absorption and to help maximize the thrust, however, its density will not add significant weight to the sail. (7:2)

In order for the sail to remain in acceptable temperature limits in space, the ratio of the solar absorbance of the sun-side coating to the sum of the emittances of the sun-side and back-side must be low, preferably below 0.2. However, even Kapton metallized by a 1000 \AA sun-side coating of highly reflective aluminum does not meet this requirement. The addition of a 100 \AA layer of chromium to the back-side becomes necessary, increasing the emittance from .34 to .64 (as seen in Figure 8), and therefore lowering the ratio to an acceptable .188. Chromium is chosen based on tests done by the California Institute of Technology on the thermal radiative properties of sail materials. (7:1-7)

The solar sail film also needs some reinforcing material necessary to avoid "billowing" and therefore loss of force, and to help control rips from micrometeoroids. The material chosen for this reinforcement is a polyamide composite tape with unidirectional graphite fibers bonded to the sail's back side in squares of ten centimeters on a side. With this reinforcement the loss of sail area from micrometeoroid tears will be as follows. (8:5)

1 Year 1.2 % x (25992) m² = 311.9 m²

2 Year 3.5 % x (25992) m² = 909.72 m²

The reinforcing structures for the sail and bus need to be lightweight and easy to pack. Several ideas considered include composite beams, plastic gas filled tubes, and aluminum beams. However, gas filled tubes were eliminated as a choice because of micrometeoroids, and aluminum beams were not practical to pack.

Composite beams are chosen for the sail's reinforcing structure because of their strength and versatility for packing. Specifically, the booms will consist of the F263 Epoxy Resin, a high temperature resin for aerospace applications produced by HEXCEL, combined with a UV activator and woven with carbon fibers into a fabric. This particular system was chosen for its non-tackiness but flexibility when uncured, and strength when cured. (10). The epoxy/carbon fabric characteristics are found in Tables 6a-d.

This fabric will form the boom by laying the prepreg fabric uncured on an elliptical steel mandrel which is first coated lightly with a Teflon release sheet. After release from the mandrel, the uncured boom is joined with the sail material with a polyester adhesive from Dupont and wrapped around the bus for storage. Normally this resin system is cured by heat but the addition of the activator will cause the curing by UV radiation after deployment. (10)

The bus materials considered are several aluminum and magnesium alloys whose properties are given in Tables 1a and 1b.

Based on the density and the minimum strength required, a magnesium alloy sheet AZ31B-H24, is chosen. The rear side of the bus is coated with silvered Teflon, because its ratio of absorbtivity to emissivity (.08/.76) is much lower than that of aluminum, and therefore will aid in thermal control of the bus.
(11:251)

Power System

A properly functioning power system is essential to the solar sail mission; without power, the electronics will not run and the motors cannot move the ballast masses to keep the sail on course. The various components of the power system include an energy source, energy conversion, energy storage and a power conditioning and control system. A schematic of the power system is shown in Figure 9.

For the solar sail mission, the energy source will be direct solar radiation which is converted into power by a .75 meter by .75 meter flat solar sail array located on the sail bus. Different types of solar cells considered include gallium arsenide and silicon cells. While silicon cells are well tested and used by most Earth orbiting spacecraft, they do exhibit several less desirable qualities than GaAs cells such as a lower efficiency (14%) and a greater degradation of performance under high temperatures and high radiation, as Figure 10 shows. The recently developed GaAs cells are promising with their 18.7% efficiency and low susceptibility to radiation; however, they do

not have silicon's proven reliability. Furthermore, they are two to five times the cost of silicon cells and they are over twice as dense. (11:81-86) As a result, the choice is made for reliable silicon cells over potentially more efficient but heavier GaAs cells.

The solar array is sized to produce the required amount of power according to several parts: the maximum required power, the angle between the sun's rays and the panels, and the efficiency of the solar panels. Other variables for the mission include: the change in the solar constant between Earth (1370 W/m^2) and Mars (590 W/m^2), and changes in solar array efficiency because of temperature changes and degradation because of radiation. For the given area of .562 square meters, the solar array at Mars will still generate the maximum power of 30 Watts under the worst possible conditions, and at the beginning of the mission, they will generate 91 Watts.

For energy storage, rechargeable batteries are used comprised of Nickel-Cadmium Cells. Nickel-Cadmium cells, although (as seen in Table 7) they do not have the highest energy density of the cell types considered, were also chosen for their reliability. From Table 8, the particular battery chosen is comprised of cells giving an ampere-hour capacity of 2 AH, an equivalent of 55 Watt-Hours, and it is made by General Electric. It is charged by the solar panels and used for energy storage and as a back-up if an emergency arises.

The power conditioning and control system uses regulators, ac-dc converters and control circuits to match the power produced by the solar cells with that required by the various sail subsystems such as telemetry, control and communications. It will also control and regulate the charging of the battery.

Attitude Control

The attitude control system can be broken down into three different categories, the attitude sensors, computer system, and the motors used to move the ballast masses. The attitude sensor system will consist of two star trackers. They will define the x-axis (pitch) and the y-axis (yaw); the z-axis (spin) will be fixed at an angle of 35 degrees with respect to the sun. A star tracker is locked onto a target star by focusing the image of the star on a photosensitive surface with an optical telescope (13:226). When the target star is not focused on the center of the photosensitive surface an error signal is sent to the computer system, which will make the necessary calculations to counter the improper rotation. The computer system will send a signal to the ballast motors, which will move the ballast masses in the proper direction and required distance along the boom.

The resultant force from the solar wind is assumed to act through the center of the solar sail. When the ballast masses are moved from their equilibrium positions, the center-of-mass for the solar sail is changed, producing a moment-arm between the resultant force and the center-of-mass which causes the moment

required to stop the unwanted angular velocity. The moment needed to produce critical yaw or pitch is much larger than that needed to produce spin. Therefore, the unwanted yaw and pitch due to inconsistencies in the sail material can be easily handled by the attitude control system. The spin due to these inconsistencies is not as troublesome since the orientation with the sun will not be affected.

Communications

The main components in the communications system will consist of a low and high gain antenna, a transmitter, and a receiver. The main purpose of the communication system is to periodically transmit the coordinates of the solar sail to the earth, about once a week. The power required by the communication system will peak at about 30 watts over a short period of time. The solar sail will be tracked by NASA's Deep Space Network.

Thermal Control

The solar sail will experience a very wide range of temperatures along the trajectory from Earth to Mars. These temperature variations will affect not only the solar sail itself, but also the electronic equipment used to control the sail and the mechanism used for deployment which involves the shape memory of the booms. The temperature effect on the sail itself is included in the choice of sail material and coating.

Solar power which involves significant heat dissipation is used to power the electronic equipment. This excess heat must be directed away from the electronic equipment, possibly by external radiator surfaces, since the electronics need to be kept within a temperature range of -5°C to 65°C , the batteries between 0°C and 20°C , and transmitter between 10°C and 60°C . (11:246) Since the electronic equipment might not be located next to an external surface, heat pipes are one way to transport the excess heat to one of the external radiator surfaces. Although the temperatures experienced near Mars are far too low for electronic equipment to withstand, this will not be a problem since the vehicle will absorb enough heat to raise the temperature of the vehicle by $.4466^{\circ}\text{C}/\text{sec}\text{-m}^2$. Thus, protecting the vehicle from very cold temperatures will be accomplished by reducing the amount of heat radiated from the surface. Since the batteries require the smallest temperature range they will also be wrapped in a thermal blanket. Heater pipes will lead from the individual components to the radiator surface. The entire buss except for the two ends will be wrapped in a thermal blanket to minimize temperature fluctuations. (11:247-251)

Trajectory

The Solar Sail is mounted as payload on a launch vehicle that is capable of placing it directly into a geosynchronous transfer orbit. Given the weight of the sail, propulsion system, and launch vehicle interface, the Titan IV would be a choice for

the launcher. (14:79) The Titan IV and its launch characteristics are given in Figure 11. The orbit will be at approximately 22,236 miles and inclined at 30 degrees. Because of the inclination the launch requires an ETR (Eastern Test Range). Once the launcher upper stage has placed the sail into its final orbit, separation will occur and the sail will coast. The next stage of the mission is one of the most important. In order to escape the gravitational attraction of Earth the solid rocket motor is fired. To intercept Mars, however, the two planets must be at the correct phase angle at the time of the impulse. The geometry of this problem is given in Figure 12. The correct phase angle for interception is 107.56 degrees. (11:154) The requirement that the phase angle be correct puts severe limitations on the times that escape can occur. The heliocentric longitude of Mars is found from the American Ephemeris and Nautical Almanac. This information is then used to determine the time of year during which the correct phase angle occurs. Once free of the Earth the deployment phase of the mission can begin. The solid rocket motor and launch vehicle interface will separate from the main bus and deployment of the sail will begin.

For planetary missions, several possible trajectories were examined. The logarithmic spiral trajectory was finally decided on for several reasons. First, from a mathematical point of view it is the simplest to model. Second, the necessary initial conditions could be met by the mission profile. These included a hyperbolic excess velocity to establish the proper velocity

direction required for insertion into the spiral trajectory.

(16:15) Finally, the spiral trajectory is very effective when compared with more complicated optimal strategies. (11:10) The spiral trajectory is achieved by maintaining the velocity vector at a constant spiral angle while also maintaining the sail's orientation with respect to the incoming radiation at a fixed value. The constant setting between the sail's outward normal and the local vertical is 35 degrees. Figure 13 shows the actual trajectory resulting in the interception of the Martian orbit. The point of closest approach is 6087 km.

Auxiliary Propulsion

The auxiliary propulsion system chosen was a solid rocket motor. The main reason for this choice is that the components of a solid rocket make it easier to separate from the main sail bus. The design characteristics of several types of solid propellants are given in Table 4. These propellants are readily available for the solar sail mission.

Another key aspect in the design of the auxiliary propulsion system is the method of separation. A system capable of sustaining large loads, high reliability, minimum weight, good survival of temperature and radiation, minimum impulse, and no debris or contamination was essential to ensure that the sail is not damaged before deployment. Table 3 lists a comparison of various separation devices. From this the ball-lock-bolt system was chosen. (16:170-178) Figure 14 is a schematic representation

of this system. The basic elements of the system are the bolt body, actuation spool, restraining collar, and the release balls and spring. The collar and bolt disengage when the actuation spool is displaced such that its reduced diameter allows the ball to retract below the outer diameter of the bolt. The spool displaces through the expansion of a gas from a gas generator and the motor and casing disengage from the force of the spring. The kinematics of this system are given in Figure 15. An arrangement for the system suited for the sail bus is shown in Figure 16.

COST ANALYSIS*

Launch Vehicle	2.000
Materials	1.000
Propulsion	0.750
Electronics	0.500
Software	0.025
Construction and Test Facilities	1.000
Personnel	0.300

*Millions of dollars

5.575

A cost analysis based upon previous studies is given in the above table. The cost of the various systems and the cost of the overall vehicle are estimated.

WEIGHT ANALYSIS

Sail	164.53 kg
Booms	62.56 kg
Bus	132.32 kg
Payload	
Antennas and Feeds	6.00 kg
Batteries	1.15 kg
Solar Arrays	2.20 kg
Ballast Motor	4.00 kg
Ballast Masses	20.00 kg
Attitude Sensors	10.00 kg
Electrical Subsystems	7.00 kg
Total Payload	50.70 kg
Rocket Motor	50.00 kg
Housing	24.00 kg
Other	6.60 kg
Total Mass of Solar Sail	487.16 kg

The total mass of the solar sail is 487.16 kg. The mass due to the payload was approximated to be 50.70 kg. (17:16) The sail, booms, and housing were calculated from the dimensions and sail material properties.

DESIGN SUMMARY

The solar sail design is dependent upon several interrelated aspects. The square sail was chosen for its speed, ease of deployment and its attitude control system. The materials for the various components of the vehicle were chosen on their material properties and the effects of the space environment on them. Since the vehicle has a 500 kg weight limitation, densities and masses were of concern in all decisions. The trajectory is such that the mission is efficient but not beyond the structural feasibility of the sail. While several aspects of the solar sail require further research and development, its design represents the potential for a successful solar sail mission in the near future. Perhaps the solar sail, because of its endless fuel supply, is a feasible alternative to chemical rockets for interplanetary travel.

LIST OF REFERENCES

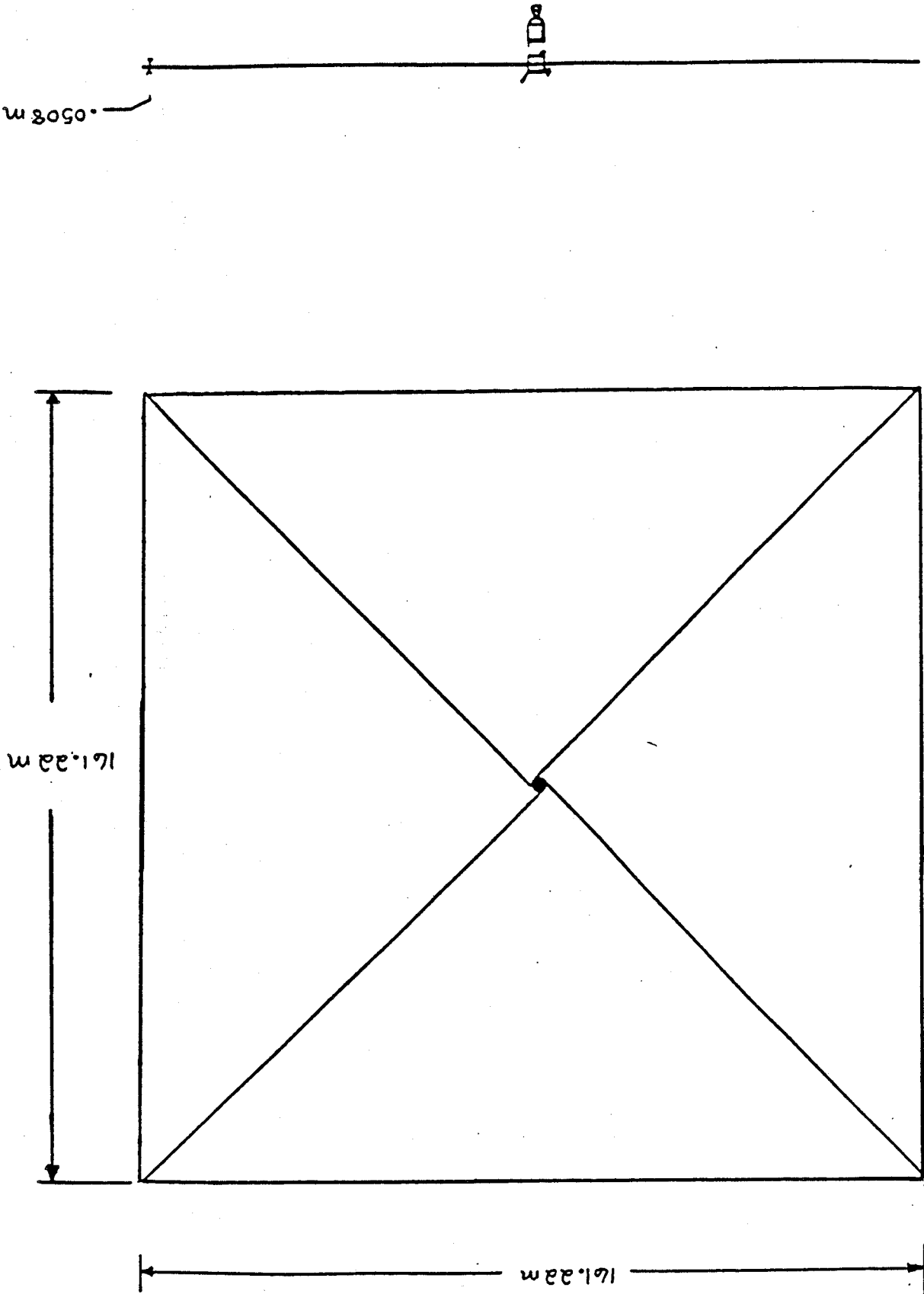
1. Svitek, T. et al, "Solar Sail As OTV /Solar Sail Concept Study- Phase II Report". American Institute of Aeronautics and Astronautics Paper 83-1347: Seattle, Washington, 1983.
2. Price, Hoppy W., "Solar Sail Engineering Development Mission", American Institute of Aeronautics and Astronautics Student Journal, vol 19. Summer 1981.
3. Tascione, Thomas F., Introduction to the Space Environment, Orbit Book Company, Malabar, Florida, 1988.
4. Giancoli, Douglas C., General Physics, Prentice-Hall Inc., Englewood Cliffs, New Jersey 07632, 1983.
5. Bate, Roger R., Fundamentals of Astrodynamics, Dover Publications, New York, 1971.
6. Linden, David, Handbook of Batteries and Fuel Cells, McGraw-Hill Book Company, New York, 1984.
7. Rowe, W.M., "Thermal Radiative Properties of Solar Sail Film Materials". American Institute of Aeronautics and Astronautics Paper 78-852: Palo Alto, California, 1978.
8. Steuer, W., "Material Problems in Solar Sail Development". American Institute of Aeronautics and Astronautics Paper 80-0315: Pasadena, California, 1980.
9. Hexcell Corporation, Properties of F264 Epoxy Resin System, 1985.
10. Dr. Gross, Auburn University Aerospace Department, (private communication), 1989.
11. Chetty, P.R.K., Satellite Technology and its Applications, Tab Books, Blue Ridge Summit, Pennsylvania, 1988.
12. Du Pont Company, Summary of Properties, Kapton Polyamide Film, 1988.
13. Corliss, William R., Space Probes and Planetary Exploration, D. Van Nostrand Company, Inc., Princeton, New Jersey, 1978.
14. Van Der Ha, J.C., "The Attainability of the Heavenly Bodies With the Aid of a Solar Sail". International Aerospace Abstracts, Germany, March 1980.

15. NASA Technical Memorandum 33-382, "Proceedings of the 3rd Aerospace Mechanisms Symposium", Jet Propulsion Laboratory, Pasadena, California, October 1968.
16. Modi, W. C., "On the Maximization of Orbital Momentum and Energy Using Solar Radiation Pressure", The Journal of the Astronomical Sciences, Volume XXVII No. 1, Jan.-March 1979.
17. Svitek, Tom, "Solar Sail Concept Study". I.A.F. Student Paper ST-82-12: Paris, France, September 1982.

FIGURES

Figure 1. Two-View Drawing of the Solar Salt

NOT TO SCALE



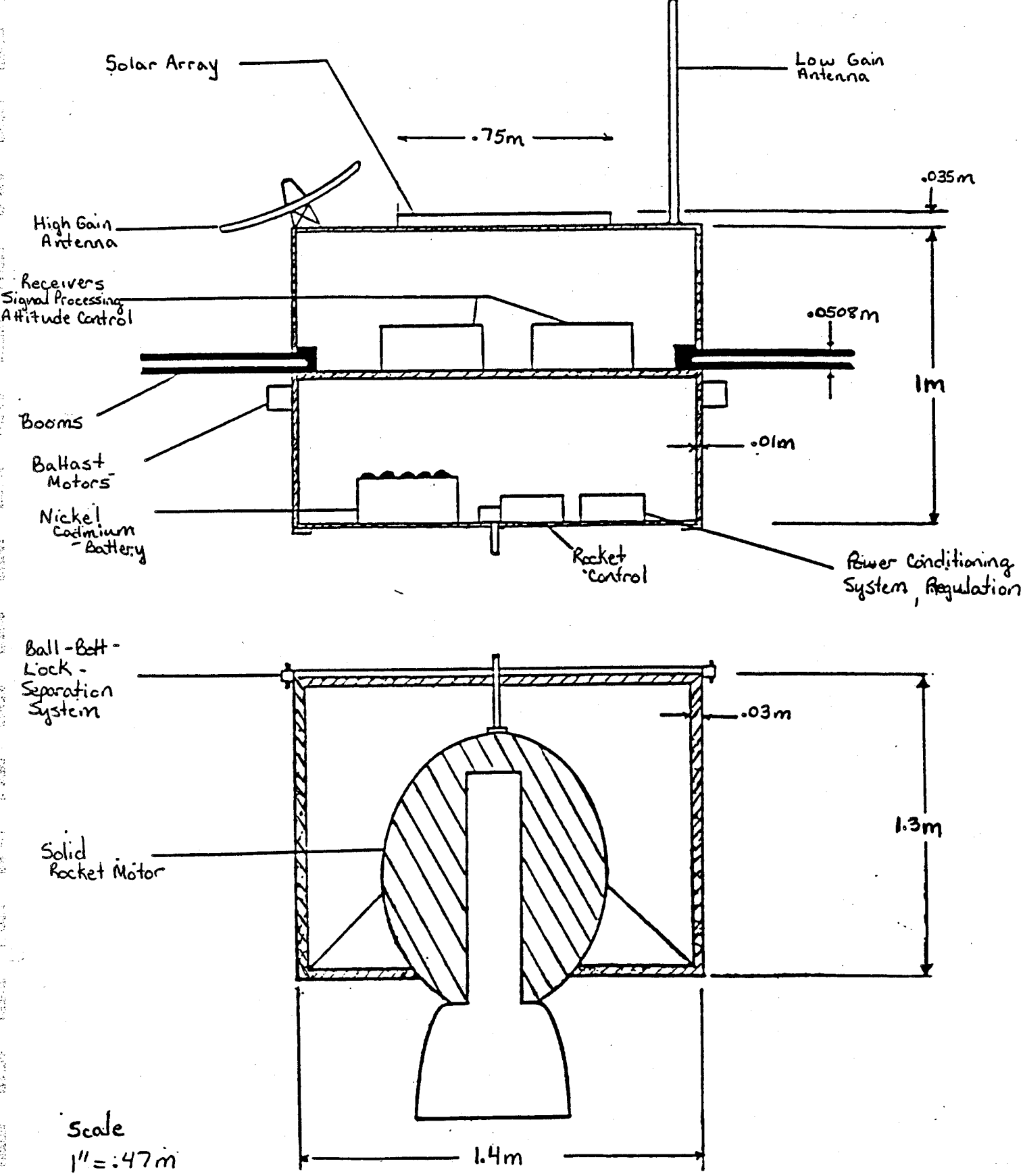


Figure 2 Cross-Sectional View of the Sail Bus

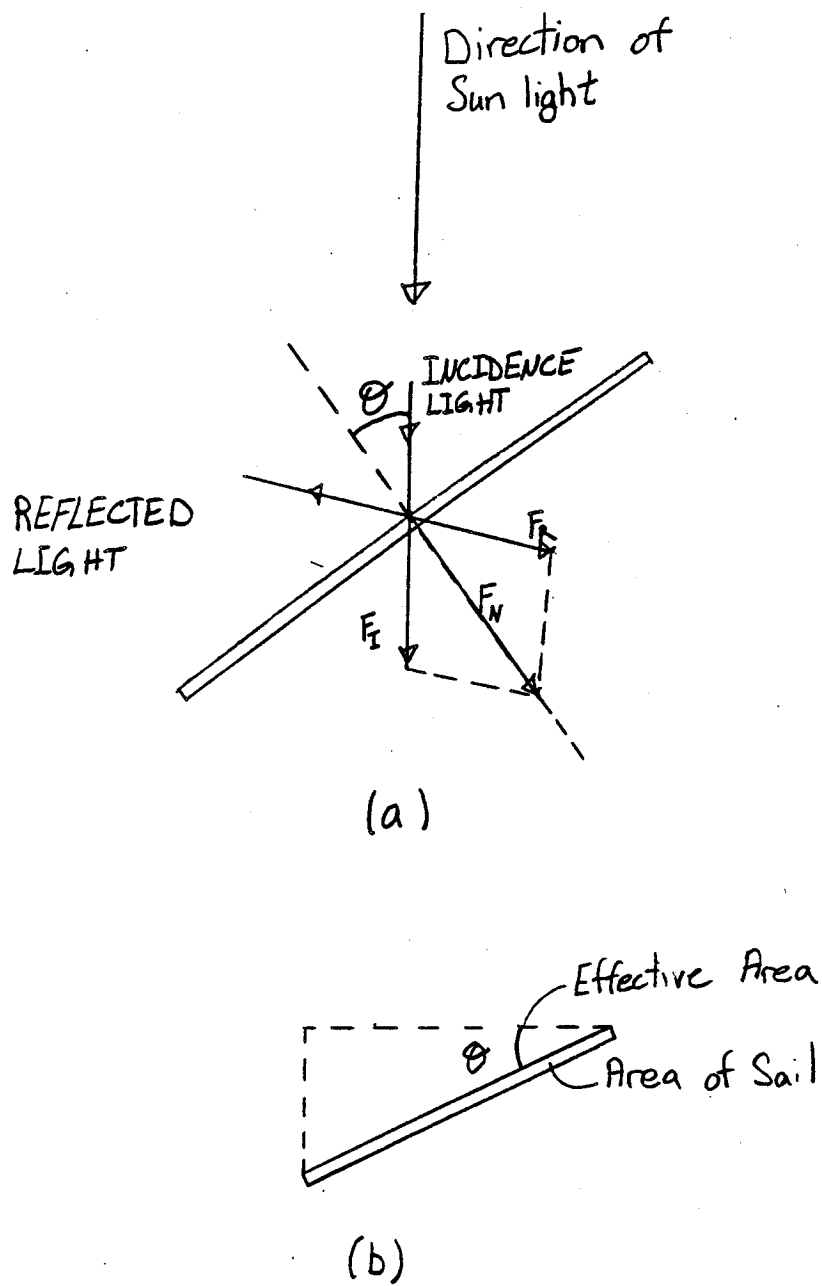


Figure 3 Solar Forces on a Reflective Surface

SOLAR CONSTANT VS. RADIUS

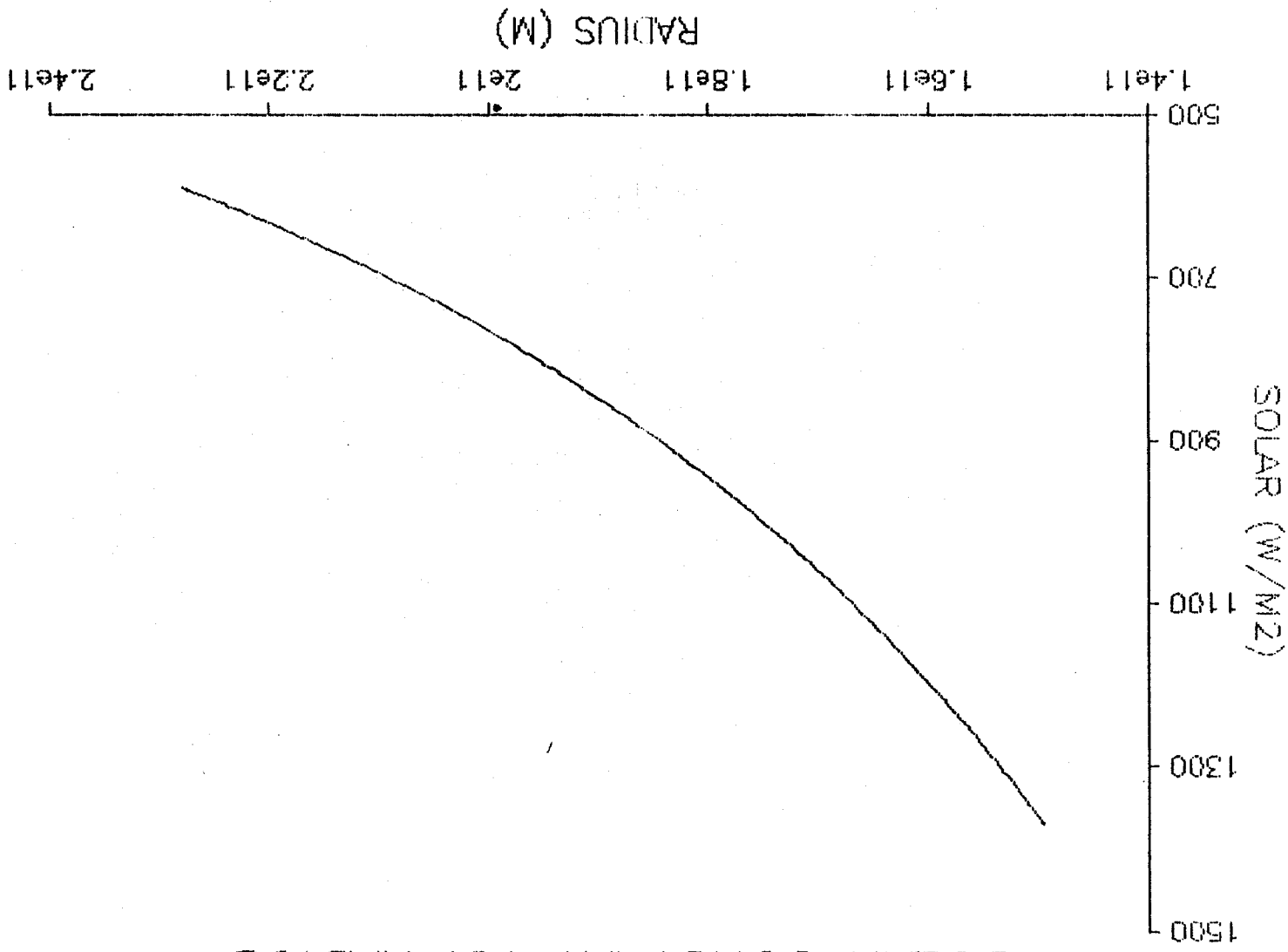


Figure 4 Solar Constant vs. Radius

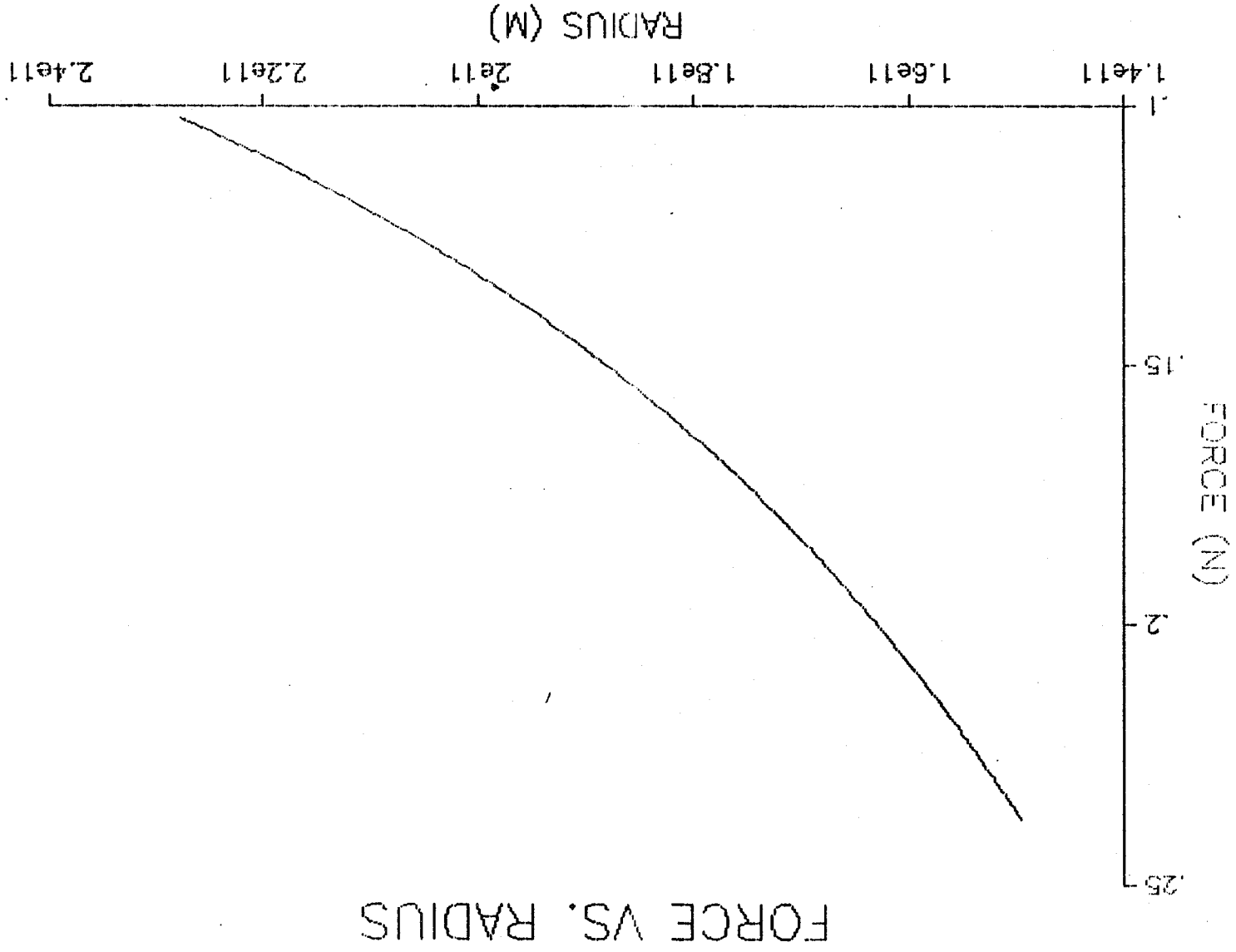


Figure 5 Solar Force vs. Radius

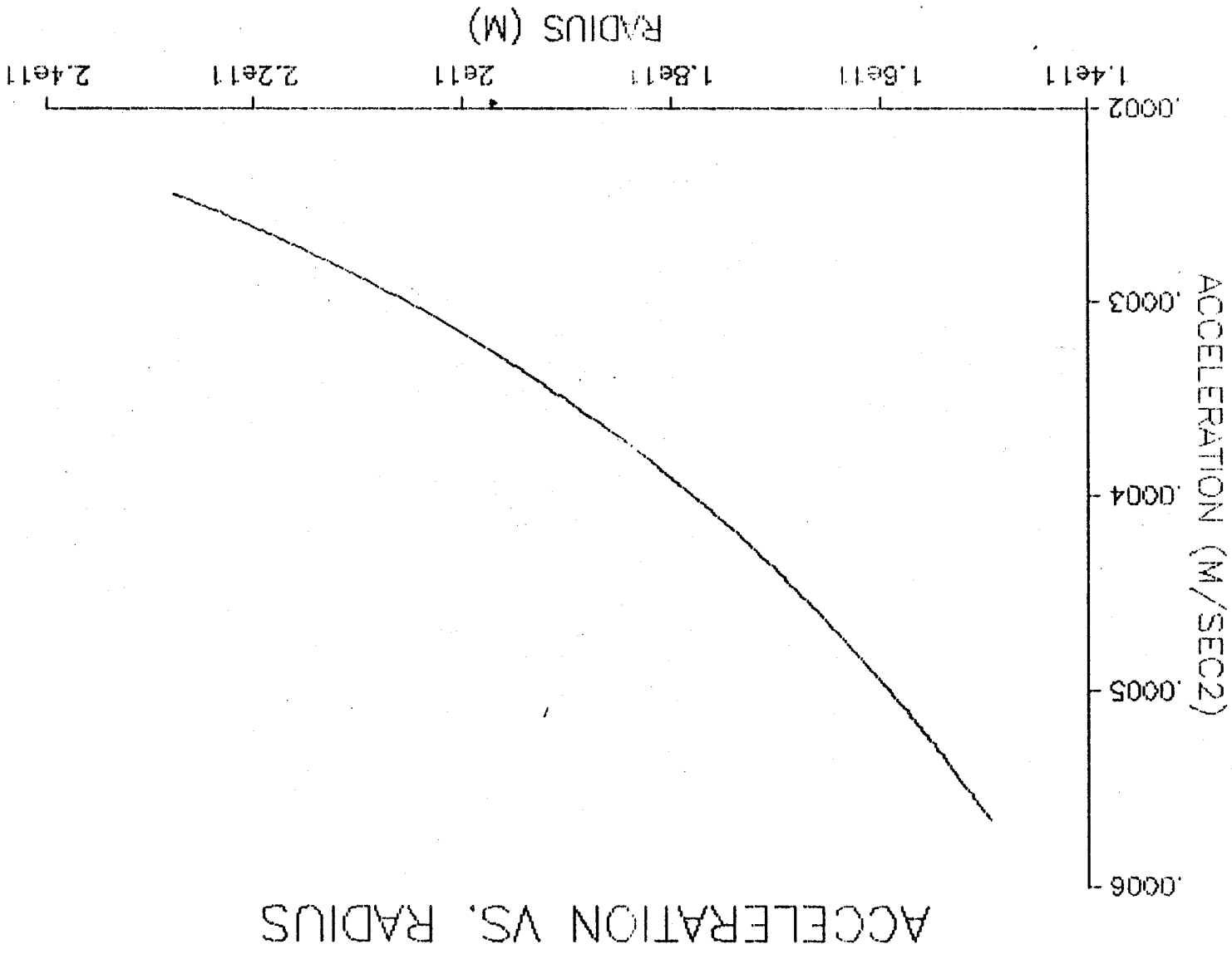


Figure 6 Acceleration of the Sail vs. Radius

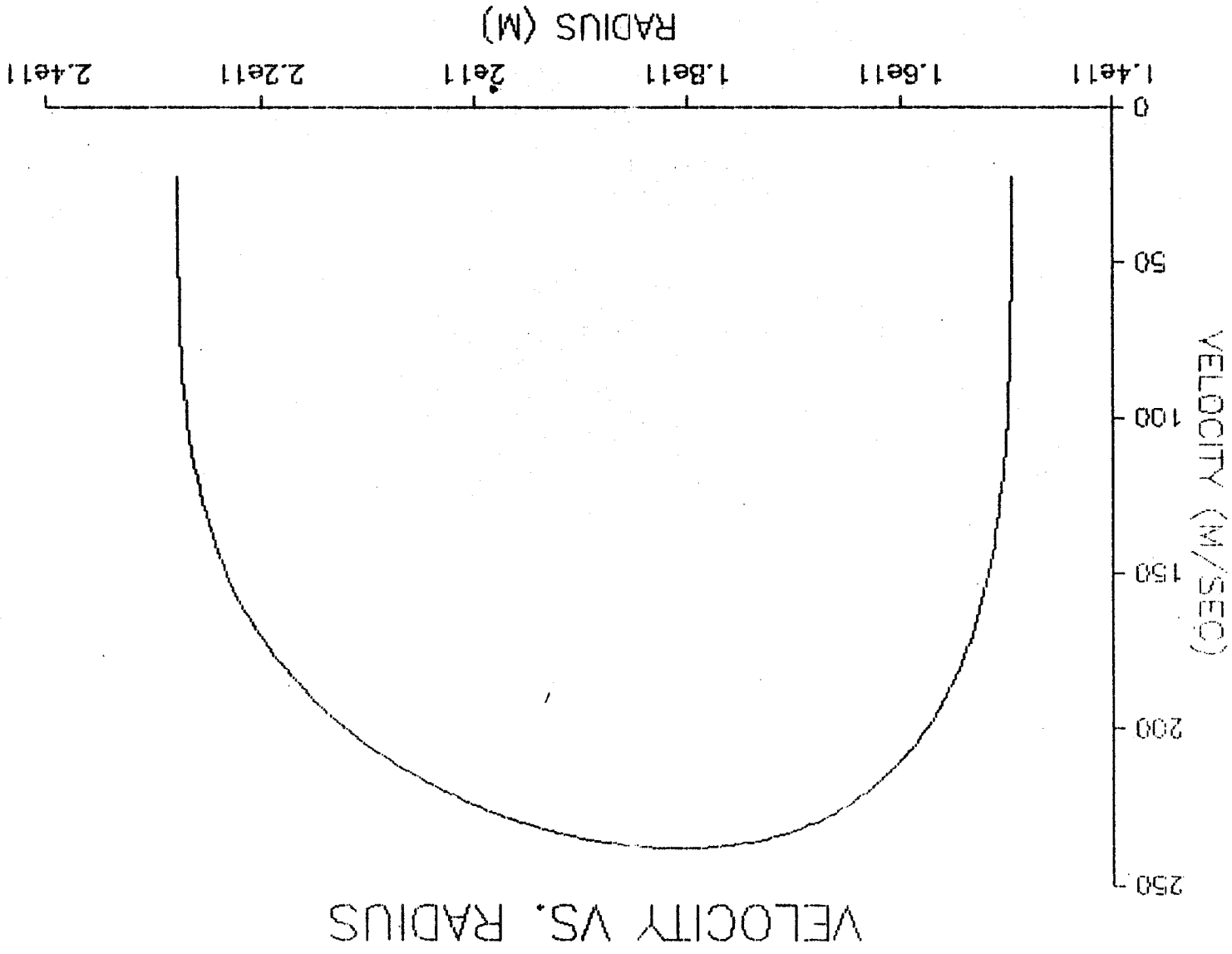


Figure 7 Velocity of the Sail vs. Radius

ORIGINAL PAGE IS
OF POOR QUALITY

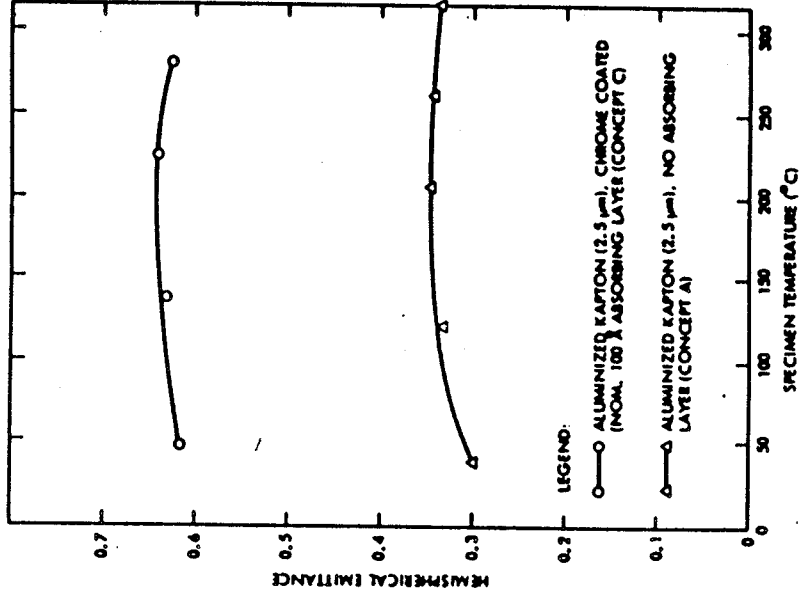


Figure 8 A Comparison of Metallized Kapton with and without a Chromium Coating. (7:5)

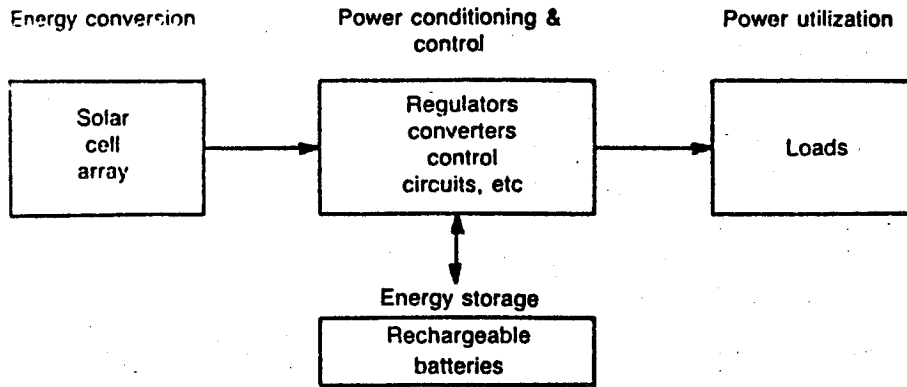


Figure 9 A Basic Spacecraft Power System (11:81)

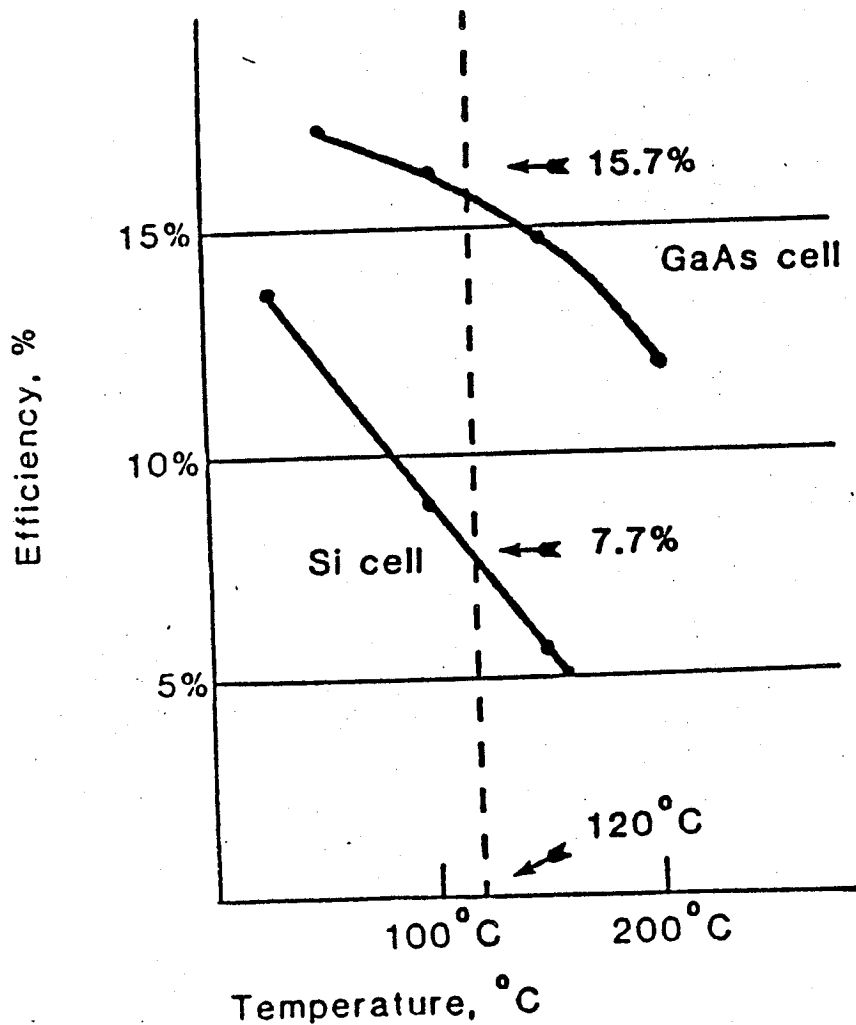


Figure 10 GaAs and Silicon Solar Cell Efficiency vs. Operating Temperatures (11:83)

Titan IV Characteristics

	Length	Diameter	Thrust	Propellants
Solid Rocket Motors (Two)	112.9 ft	10.0 ft	1.6-Million lb per Motor	Solid
Stage One	85.5 ft	10.0 ft	546,000 lb	Storable Liquid
Stage Two	32.6 ft	10.0 ft	104,000 lb	Storable Liquid
Centaur Upper Stage	29.3 ft	14.2 ft	33,000 lb	Cryogenic

Guidance: Inertial with Digital Computer
 Payload Fairing: 200-in. Diameter, 86-ft Length, Tri-Sector Design, Isogrid Construction

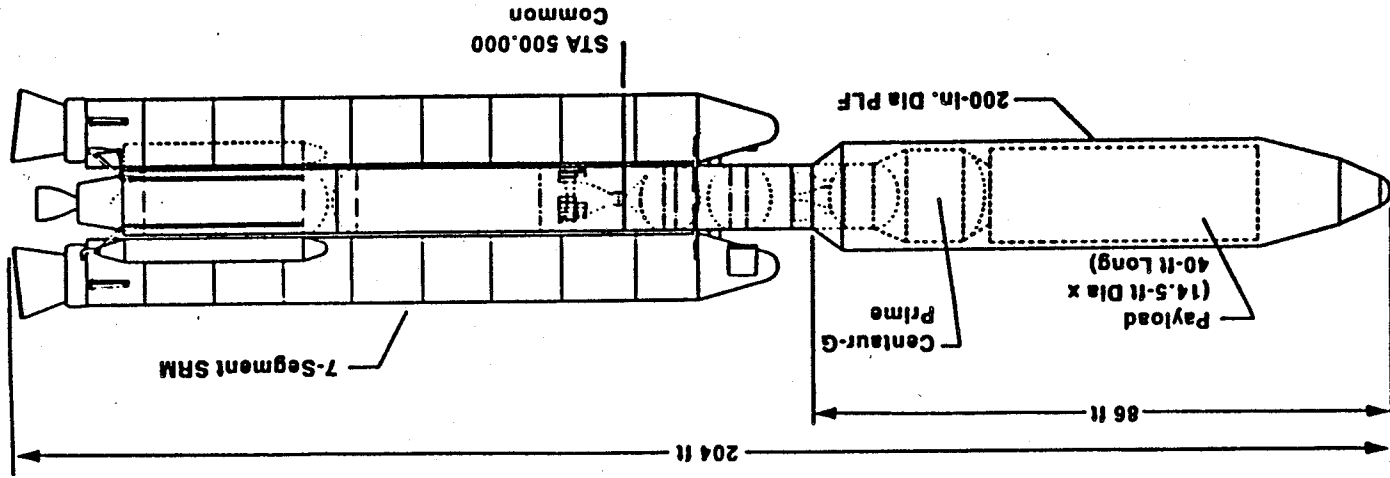


Figure 11 Titan IV Characteristics

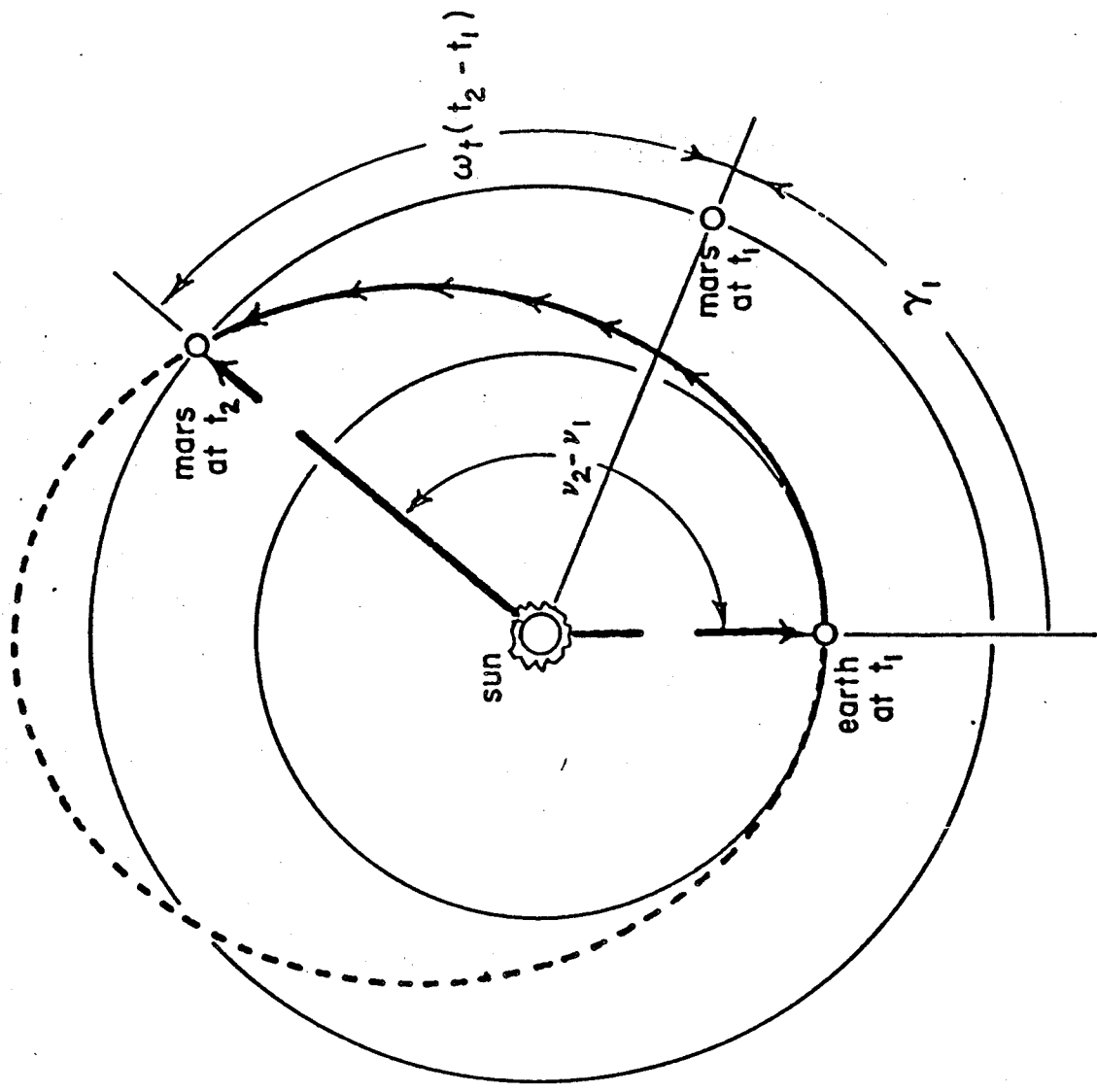


Figure 12 Departure Phase Angle for Mars Intercept

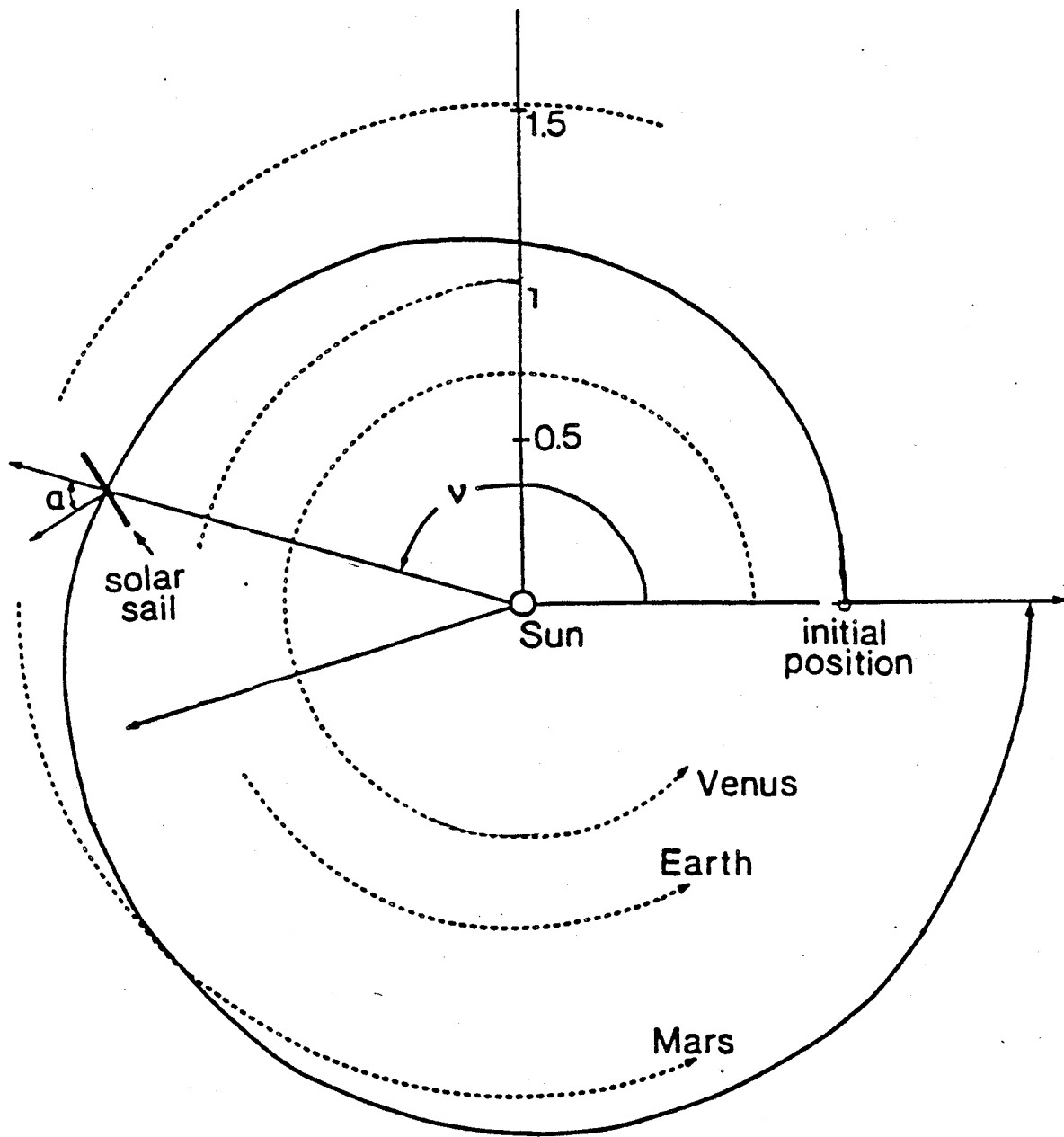


Figure 13 Interplanetary Trajectory for Constant Sail Angle Showing Interception of Martian Orbit.

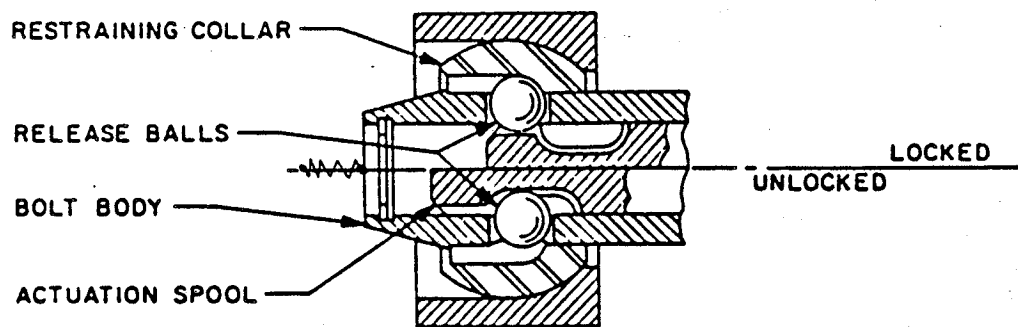
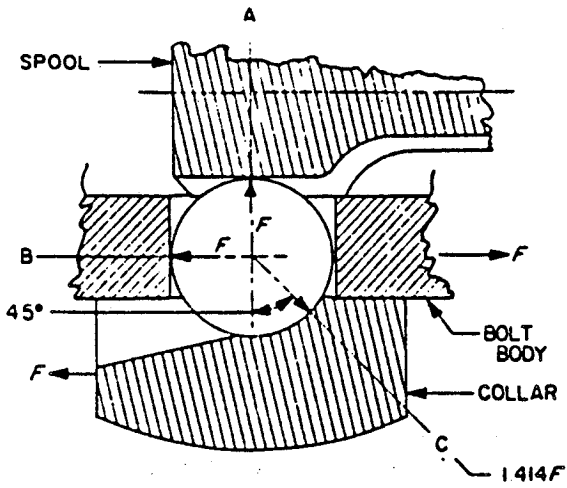
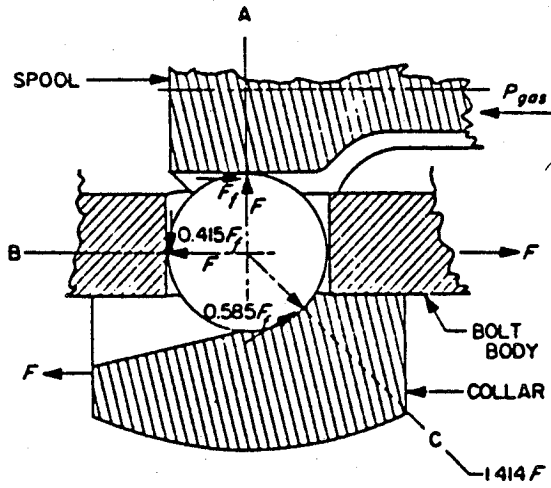


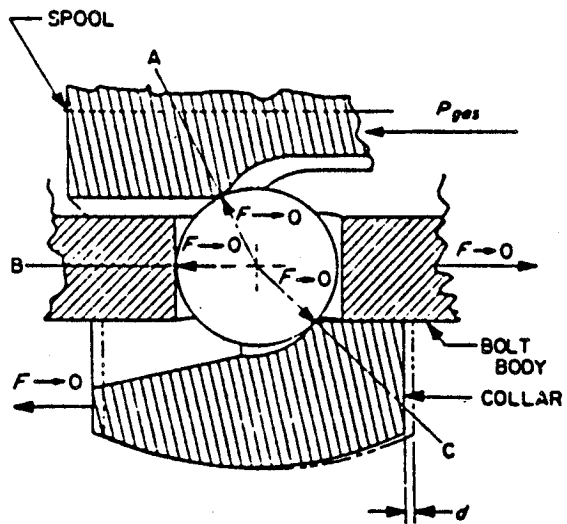
Figure 14 Schematic of Ball-Lock-Bolt Separation Mechanism
 (16:174)



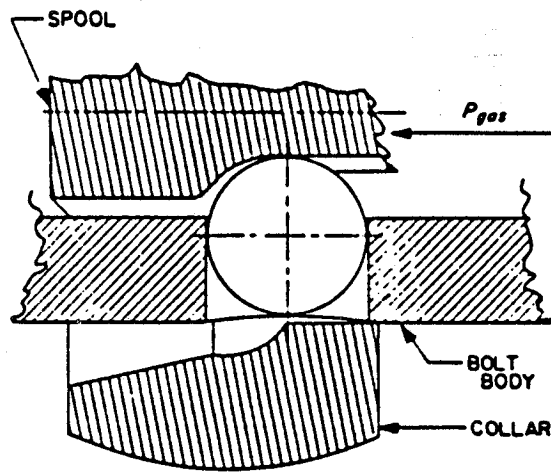
(a) STATIC LOADS



(b) STATIC LOADS PLUS FRICTION LOADS



(c) RELEASE ACTION



(d) RELEASE COMPLETE

DIMENSIONS IN INCHES

Figure 15 Kinematics of Ball-Lock-Bolt Separation Mechanism

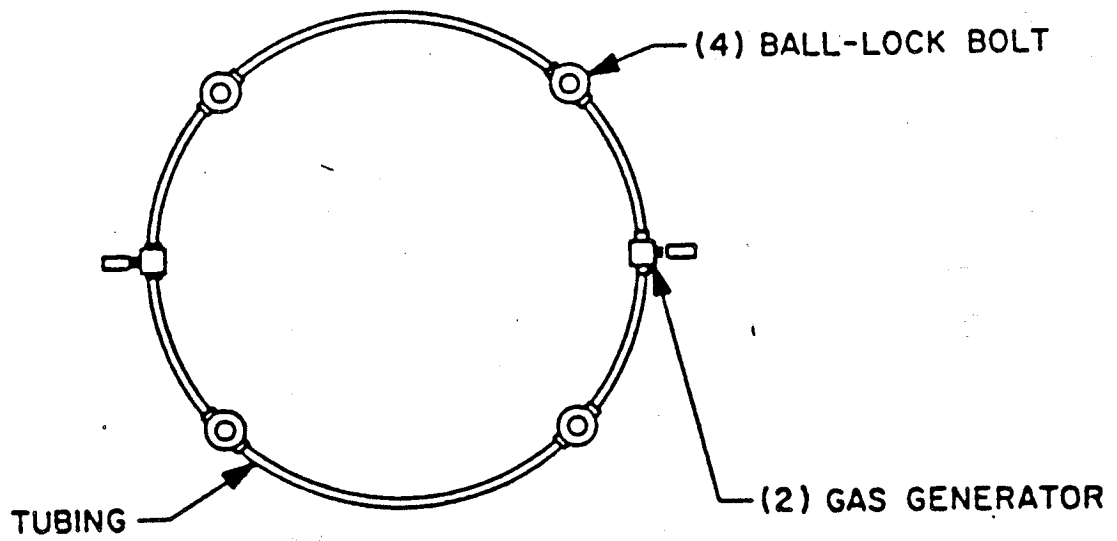


Figure 16 Arrangement of Gas-Generator and Ball-Lock-Bolt Separation System for the Sail Bus

TABLES

PRECEDING PAGE BLANK NOT FILMED

Materials	Type	Specific Heat J/kg K	Thermal Expansion 10 ⁻⁶ /K	Thermal Conductivity w/m K
Aluminum Alloy Sheet	2024-T36	880	22.5	120
Sheet	7075-T6	840	22.9	140
Beryllium Extrusion	Be-38% AL	1860	11.5	180
Lockalloy		—	16.9	210
Graphite/Epoxy, V, 55% [0]	HTS	—	-0.4	—
	UHM	—	-1.04	—
Invar 36	Annealed	510	1.3	13.5
Magnesium Sheet	AZ31B-H24	1050	25.2	97
Steel PH15-7	RH1050	—	11.0	15
Ti6AL-4V Sheet		500	8.8	7.4

PRECEDING PAGE BLANK NOT FILMED

43-44

Table 1b. Thermal Properties of Various Spacecraft Materials

(11:77)

Materials	Density Kg/m ³	Transverse ultimate tensile strength N/mm ²	Longit. ultimate tensile strength N/mm ²	Longit. tensile yield N/mm ²	Fracture Toughness (N/m ^{3/2} x 10 ⁴)
Aluminum Alloy Sheet (2024-T36)	2770	—	480	410	36
Sheet (7075-T6)	2800	—	520	450	30
Beryllium Extrusion Lockalloy (Be-38% A1)	1850	—	620	410	—
	2100	—	427	430	—
Graphite/Epoxy, V, 55% [0] HTS	1490	67	1340	—	—
[0, +/- 45]HTS	1490	290	640	—	—
Invar 36 Annealed	8080	—	490	280	—
Magnesium Sheet (AZ31B-H24)	1770	280	270	200	—
Steel PH15-7 (RH1050)	7670	—	1310	1200	—
Ti6AL-4V Sheet	4430	—	1100	1000	46

Materials	Shear Modulus N/mm ²	Young's Modulus N/mm ²	Specific Strength (Km/s) ²	Specific Stiffness (Km/s) ²
Aluminum Alloy Sheet (2024-T36)	28000	72000	0.17	26
Sheet (7075-T6)	27000	71000	0.19	25
Beryllium Extrusion Lockalloy (Be-38% A1)	140000	290000	0.33	158
	—	190000	0.20	88
Graphite/Epoxy, VI 55% [0] HTS	5900	150000	0.89	100
[0, +/- 45]HTS	—	83000	0.43	56
Invar 36	56000	145000	0.06	18
Magnesium Sheet (AZ31B-H24)	16000	45000	0.15	25
Steel PH15-7 (RH1050)	76000	200000	0.17	26
Ti6AL-4V Sheet	43000	110000	0.25	25

Table 1a. Mechanical Properties of Various Spacecraft Materials

(11:76)

- 47 -

Table 2. Properties of Unidirectional Advanced Composites
(12:149)

Properties of unidirectional advanced composites

Property	Boron/ epoxy	Boron/ polyimide	S-glam/ epoxy	High-modulus graphite/ epoxy	High-modulus graphite/ polyimide	High-strength graphite/ epoxy(a)	Aramid/ epoxy(b)	High-strength graphite/ epoxy(c)
Reinforcement content, vol %	50	49	72	45	45	70	54	60
Density, g/cm ³ (lb/in. ³)	2.02 (0.073)	1.99 (0.072)	2.13 (0.077)	1.55 (0.056)	1.55 (0.056)	1.61 (0.058)	1.36 (0.049)	1.58 (0.057)
Tensile strength, MPa (ksi):								
Longitudinal	1370 (199)	1040 (151)	1290 (187)	840 (122)	807 (117)	1500 (218)	1190 (172)	1520 (220)
Transverse	56 (8.1)	11 (1.6)	46 (6.7)	42 (6.1)	15 (2.2)	40 (5.8)	11 (1.6)	55 (8.0)
Tensile modulus, GPa (10 ⁶ psi):								
Longitudinal	201 (29.2)	221 (32.1)	61 (8.8)	190 (27.5)	216 (31.3)	145 (21.0)	84 (12.2)	110 (16.0)
Transverse	22 (3.2)	14 (2.1)	25 (3.6)	6.9 (1.0)	5.0 (0.72)	10 (1.5)	4.8 (0.70)	15 (2.2)
Compressive strength, MPa (ksi):								
Longitudinal	1600 (232)	1090 (158)	820 (119)	883 (128)	652 (94.5)	1700 (247)	290 (42)	1240 (180)
Transverse	123 (17.9)	63 (9.1)	162 (23.5)	197 (28.5)	70 (10.2)	246 (35.7)	65 (9.4)	248 (36.0)
Shear modulus, GPa (10 ⁶ psi)	5.38 (0.78)	7.65 (1.11)	12.0 (1.74)	6.2 (0.9)	4.48 (0.65)	6.9 (1.0)	2.83 (0.41)	4.96 (0.72)
Intralaminar shear strength, MPa (ksi)	63 (9.1)	26 (3.8)	45 (6.5)	61 (8.9)	22 (3.2)	68 (9.8)	28 (4.0)	69 (10.0)
Poisson's ratio:								
Major	0.17	0.16	0.23	0.10	0.25	0.28	0.32	0.25
Minor	0.02	0.02	0.09	...	0.02	0.01	0.02	0.034
Moisture coefficient, 10 ⁻³ mm (10 ⁻³ in.):								
Longitudinal	0.0762 (0.003)	0.0762 (0.003)	0.3556 (0.014)	0.0762 (0.003)	0.0762 (0.003)	0.1524 (0.006)	0.2032 (0.008)	0.1524 (0.006)
Transverse	4.267 (0.158)	4.267 (0.168)	3.251 (0.128)	3.277 (0.129)	3.277 (0.129)	3.277 (0.129)	3.835 (0.151)	3.277 (0.129)
Coefficient of thermal expansion, 10 ⁻⁴ /°C (10 ⁻⁴ /°F):								
Longitudinal	6.1 (3.4)	4.9 (2.7)	3.8 (2.1)	...	0.0 (0.0)	0.02 (0.01)	-2.88 (-1.60)	0.72 (0.40)
Transverse	30.4 (16.9)	28.4 (15.8)	16.7 (9.3)	33.3 (18.5)	25.4 (14.1)	22.5 (12.5)	56.3 (31.3)	29.5 (16.4)

(a) Union Carbide Thornel 300 fibers. (b) Du Pont Kevlar 49. (c) Hercules AS fibers.

Source: Ref 4, p 36

ORIGINAL PAGE IS
OF POOR QUALITY

Requirement	Linear explosive	Contained linear explosive	Explosive bolts/nuts	Ball lock	V-band	Pin puller	Cable cutter	Collet mechanism
Load capability	E	G	E	G	E	G	G	E
Uniform load	E	E	G	G	E	P	P	G
Minimum shock	P	P	G	E	E	P	G	E
Minimum impulse	P	P	P	E	E	E	E	E
Minimum tip-off	P	P	G	E	G	E	E	E
Minimum electrical power	E	E	P	G	E	P	P	G
Compatibility with structure	G	P	E	E	G	G	G	E
No contamination	P	E	P	E	E	E	E	E
No debris	P	E	P	E	G	E	E	E
Maintainability	P	P	G	E	E	G	G	E
Reusability	P	P	P	E	E	P	P	E
Safety	P	P	G	E	E	E	E	E
Long life in space	P	P	E	E	G	G	E	E
Long life in storage	E	G	E	E	E	E	E	E
High reliability	G	G	E	E	E	E	P	E
Minimum weight	P	P	E	G	G	E	G	G
Minimum volume	G	G	E	G	G	G	E	P
Survival of temperature extremes	P	P	P	E	G	G	G	E
Survival of radiation	P	P	G	E	E	E	E	E

NOTE: E = Excellent, G = Good, P = Poor.

Table 3. Comparison of Vehicle Separation Mechanisms

48A

Property	Extruded JPN ballistite	Asphalt-base thermoplastic composite	NDRC molded composite
Specific impulse, sec	220	186	170
Exhaust velocity, ft/sec	7100	6000	5500
Density, lb _m /ft ³	101.5	110	100 to 115
Specific impulse/unit volume, %	100	96	80 to 90
Burning rate, in/sec	1.4	1.6	0.25 to 1.32
Burning-rate exponent	0.73	0.76	0.40
Area ratio**	185	175	200 to 1000
Low-pressure combustion limit, psia	500	1000	No lower limit
Flame temperature, °F	5300	3000	3000
Exhaust jet	Smokeless	Smoky	Smoky

Table 4. Characteristics of Some Solid Propellants

KAPTON® Type 100 HN Film 25 μm (1 mil)

PHYSICAL PROPERTIES

PHYSICAL PROPERTIES	TYPICAL VALUES		TEST METHOD
	23°C (73°F)	200°C (392°F)	
Ultimate Tensile (MD) Strength, MPa (psi)	231 (33,500)	139 (20,000)	ASTM D-882-83, Method A ¹
Yield Point (MD) at 3%, MPa (psi)	69 (10,000)	41 (6,000)	ASTM D-882-81
Stress to Produce (MD) 5% Elongation, MPa (psi)	90 (13,000)	61 (9,000)	ASTM D-882-81
Ultimate Elongation (MD), %	72	83	ASTM D-882-81
Tensile Modulus, GPa (MD) (psi)	2.5 (370,000)	2.0 (290,000)	ASTM D-882-81
Impact Strength, Kg-cm (ft-lb)	8 (.50)		Du Pont Pneumatic Impact Test
Folding Endurance (MIT), cycles	285,000		ASTM D-2176-69 (1982)
Tear Strength (MD) - Propagating (Elmendorf), g	7		ASTM D-1922-67 (1978)
Tear Strength (MD) - Initial (Graves), g	729		ASTM D-1004-66 (1981)
Density, g/cm ³	1.42		ASTM D-1505-68 (1979)
Coefficient of Friction - Kinetic (Film-to-Film)	.48		ASTM D-1894-78
Coefficient of Friction - Static (Film-to-Film)	.63		ASTM D-1894-78
Refractive Index (Becko Line)	1.66		ASTM D-542-50 (1977)
Poisson's Ratio	.34		Avg. 3 Samples Elongated at 5%, 7%, 10%
Low Temperature Flex Life	Pass		IPC TM 650, Method 2.6.18

(MD) - Machine Direction
¹Specimen Size: 25 x 170mm (1" x 6"); Jaw Separation: 100mm (4"); Jaw Speed: 50mm/min (2"/min); Ultimate refers to the tensile strength and elongation measured at break.

Table 5a. Properties of Kapton

(12:4)

E (GN/m ²)	3%	
	Yield Strength (MN/m ²)	Ultimate Strength (MN/m ²)
3.5	-	240
3.0	69	170
1.8	41	120

Table 5b. Strength of Kapton

(6:465)

NEAT RESIN PROPERTIES

SPECIFIC GRAVITY	1.267 g/cc
T _g WET	271 °F
T _g DRY	370 °F
EQUILIBRIUM MOISTURE ABSORPTION	4.8%
LINEAR COEFFICIENT OF THERMAL EXPANSION	2.9 x 10 ⁻⁵ in/in/°F
TENSILE STRENGTH	10.9 ksi
TENSILE MODULUS	0.62 msi
TENSILE STRAIN	2.4%
FRACTURE TOUGHNESS, K _{IC}	0.55 ksi $\sqrt{\text{in}}$
	0.60 MPa $\sqrt{\text{m}}$
STRAIN ENERGY RELEASE RATE, G _{IC}	0.43 lb/in
	0.075 KJ/m ²
GEL TIME @ 350 °F	2-9 min.

Table 6a. Epoxy Resin F263 Properties (9:2)

NOTE: ALTERNATE CARBON AND GLASS FABRIC WEAVES MAY BE USED WITH THE F263 RESIN SYSTEM. ALSO, F263 CARBON TAPES MAY BE PRODUCED WITH VARIOUS CARBON FIBER TYPES AND TOW SIZES. IN DESIGNATING TAPE, THE SECOND DIGIT REPRESENTING TOW SIZE AND THE THIRD DIGIT REPRESENTS FIBER SOURCE. CONSULT YOUR NEAREST HEXCEL REPRESENTATIVE FOR ADDITIONAL INFORMATION.

FORM	HEXCEL DESIGNATION	FIBER	FIBER AREAL WT. g/m ²	WEAVE	COUNT WARP x FILL	STANDARD WIDTH	AVAILABLE WIDTHS
CARBON FABRIC	W3T282-42-F263	T300 CELION	194	PLAIN	12.5 x 12.5	42"	—
	F3T584-42-F263	T300 CELION	370	8 HARNES SATIN	24 x 24	42"	—
GLASS FABRICS	120-38-F263	450%	115	CROWFOOT MIL-C-9084TYIII	60 x 58	38"	44", 50", 60"
	1581-38-F263	150%	303	8 HARNES SATIN MIL-C-9084TYVIII	57 x 54	38"	44", 50", 60", 72"
	7781-F263	75%	303	8 HARNES SATIN MIL-C-9084TYVIII	57 x 54	38"	44", 50", 60", 72"
CARBON TAPES	T--095-12-F263	VARIOUS	95	NA	NA	12"	3" - 24"
	T--145-12-F263	VARIOUS	145	NA	NA	12"	3" - 24"
	T--190-12-F263	VARIOUS	190	NA	NA	12"	3" - 24"

AVAILABILITY

Table 6b. Epoxy Resin F263 Availability (9:3)

Table 6c. Carbon Fabric Physical Properties (9:3)

PHYSICAL PROPERTIES

	PROPERTY	CARBON FABRICS		CARBON TAPES			GLASS FABRICS	
		W3T282 OR W3C282	F3T584 OR F3C584	95 g/m ²	145 g/m ²	190 g/m ²	120	7781
PREPREG	MATERIAL DESCRIPTION							
	% FLOW @ 350° F 50 psi	9-22%	9-22%	11-24%	11-24%	11-24%	15-30%	10-30%
	% RESIN CONTENT (DRY)	38-42	35-39	35-39	35-39	35-39	42-48	36-40
LAMINATE	CURED THICKNESS PER PLY (IN)	0.0072	0.0135	0.0039	0.0059	0.0078	0.0045	0.010
	% FIBER VOLUME	61	62	55	55	55	38	45

-57-

LAMINATE MECHANICAL PROPERTIES

PROPERTY	TEMP	CARBON FABRICS		CARBON TAPES			GLASS FABRICS	
	°F	W3T282	F3T584	T3T095	T3T145	T3T190	120	7781
TENSILE STRENGTH, KSI	75	82.6	88.4	180.8	197.5	196.3	53.4	66.9
TENSILE MODULUS, MSI	75	8.81	9.24	19.55	19.19	19.12	3.47	4.30
TENSILE STRAIN, $\frac{u}{in}$	75	9,762	10,024	9,267	10,345	10,142		
TENSILE STRENGTH, KSI	350	78.5	84.0		187.6		38.1	55.8
TENSILE MODULUS, MSI	350	8.37	8.78		18.23		2.94	3.46
COMPRESSION STRENGTH, KSI	75	94.0	96.6	206.0	193.3	175.8	68.7	71.2
COMPRESSION MODULUS, MSI	75						3.41	4.36
COMPRESSION STRENGTH, KSI	160	83.4	84.9	182.7	167.4	171.8		
COMPRESSION STRENGTH, KSI	350						50.0	51.2
COMPRESSION MODULUS, MSI	350						3.11	3.83
SHORT BEAM SHEAR, KSI	-65	10.50	9.46	18.92	17.99	17.76		
SHORT BEAM SHEAR, KSI	75	10.72	10.40	16.06	16.16	15.92		
SHORT BEAM SHEAR, KSI	270	8.05	6.99	10.87	10.48	10.96		
SHORT BEAM SHEAR, KSI	350	6.73	6.88		9.82			
INTERLAMINAR SHEAR, KSI	75						2.99	3.37
INTERLAMINAR SHEAR, KSI	350						2.24	2.61

Table 6d. Carbon Fabric Laminate Mechanical Properties (9:4)

-52-

Table 7. Characteristics of Different Storage Cells (11:107)

Type of Cells	Electrolyte	Nominal Voltage/ Cell (Volts)	Energy Density (Whr.kg)	Temperature (Deg C)	Cycle Life at Different Depth of Discharge Levels			Whether Space Qualified
					25%	50%	75%	
Ni-Cd	Diluted Potassium Hydroxide (KOH) solution	1.25	25-30	-10 - 40	21000	3000	800	Yes
Ni-H ₂	KOH solution	1.30	50-80	-10 - 40	>15000	>10000	>4000	Yes*
Ag-Cd	KOH solution	1.10	60-70	0 - 40	3500	750	100	Yes
Ag-Zn	KOH solution	1.50	120-130	10 - 40	2000	400	75	Yes
Ag-H ₂	KOH solution	1.15	80-100	10 - 40	>18000	—	—	No
Pb-Acid	Diluted sulfuric acid	2.10	30-35	10 - 40	1000	700	250	—

*Ni-H₂ cells are employed on-board the Navigational Technology Satellite (NTS-2) and other geosynchronous satellites. However, these cells have not been used on any low earth orbit satellites.

-53-

ORIGINAL PAGE IS
OF POOR QUALITY

GENERAL ELECTRIC NICKEL-CADMIUM SATELLITE CELLS

Standard Cells

Size (Ah) Capacity	Catalog Number 4280—	A Height	B Overall Height	C Base Width	D Base Lg.	Neg. Plate Treat	Weight (Grams) Calc. Max.
1	01AB01	1.560	1.695	.402	1.295	—	50
2	02AB03	1.790	2.200	.650	2.000	Ag	115
3	03AB07	2.030	2.483	.813	2.117	—	155
4	04AB36	2.330	2.790	.830	2.137	Ag	190
5	05AB01	2.710	3.159	.831	2.132	Ag	230
6	06AB49	3.180	3.640	.846	2.155	Ag	2080
7	07AB09	3.500	3.960	.831	2.132	Ag	310
6	08AB05	2.800	3.406	.891	2.988	Ag	380
10	10AB08	3.330	3.926	.891	2.988	Ag	455
12	12AB24	4.030	4.630	.903	3.000	Ag	585
15	15AB19	4.720	5.320	.891	2.988	Ag	670
17	24AB01	4.534	5.134	.650	2.988	Tfe	635
20	24AB05	6.350	6.950	.651	2.988	Tfe	950
20	24AB03	6.530	7.136	.903	3.000	Ag	935
24	24AB02	4.720	5.320	.891	3.763	Ag	845
30	30AB10	7.130	7.726	.903	3.000	Tfe	1115
50	50AB12	5.650	6.250	1.297	5.007		2000
100	100AB52	7.290	8.200	1.522	7.177		4020

Nickel cadmium cells
for satellite applications

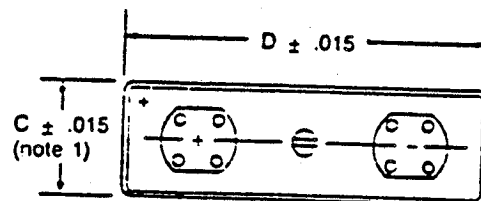


Table 8. General Electric Nickel-Cadmium Satellite Cells

(11:142)